ResearchGate

See discussions, stats, and author profiles for this publication at: https://www.researchgate.net/publication/8351558

Microfluidic T-Form Mixer Utilizing Switching Electroosmotic Flow

ARTICLE *in* ANALYTICAL CHEMISTRY · OCTOBER 2004

Impact Factor: 5.64 · DOI: 10.1021/ac0494782 · Source: PubMed

CITATIONS
59

READS
33

3 AUTHORS, INCLUDING:

Che-Hsin Lin
National Sun Yat-sen University
153 PUBLICATIONS **2,272** CITATIONS
SEE PROFILE

Lung-Ming Fu
National Pingtung University of Science and…
134 PUBLICATIONS **2,510** CITATIONS
SEE PROFILE

Available from: Che-Hsin Lin
Retrieved on: 03 February 2016

Anal. Chem. **2004,** *76,* 5265−5272

Microfluidic T-Form Mixer Utilizing Switching Electroosmotic Flow

Che-Hsin Lin,[†] Lung-Ming Fu,*[,‡] and Yu-Sheng Chien[†]

Department of Mechanical and Electromechanical Engineering, National Sun Yat-sen University, Kaohsiung, Taiwan 804, and Graduate Institute of Materials Engineering, National Pingtung University of Science and Technology, Pingtung, Taiwan, 912

This paper presents a microfluidic T-form mixer utilizing alternatively switching electroosmotic flow. The microfluidic device is fabricated on low-cost glass slides using a simple and reliable fabrication process. A switching DC field is used to generate an electroosmotic force which simultaneously drives and mixes the fluid samples. The proposed design eliminates the requirements for moving parts within the microfluidic device and delicate external control systems. Two operation modes, namely, a conventional switching mode and a novel pinched switching mode, are presented. Computer simulation is employed to predict the mixing performance attainable in both operation modes. The simulation results are then compared to those obtained experimentally. It is shown that a mixing performance as high as 97% can be achieved within a mixing distance of 1 mm downstream from the T-junction when a 60 V/cm driving voltage and a 2-Hz switching frequency are applied in the pinched switching operation mode. This study demonstrates how the driving voltage and switching frequency can be optimized to yield an enhanced mixing performance. The novel methods presented in this study provide a simple solution to mixing problems in the micro-total-analysis-systems field.

When compared to conventional analytical techniques, microfluidic devices provide many advantages, including a more rapid detection capability, higher resolution, less sample consumption, superior portability, and disposability. Such devices have had a substantial impact on clinical analysis practices and in industrial applications in the food and chemical industries, etc. The small flow channels incorporated in microfluidic systems increase the surface-to-volume ratio and are advantageous in many applications; however, the characteristic Reynolds number for liquids flowing in these microchannels is very small (typically <10). At such low Reynolds numbers, turbulent mixing does not occur and homogenization of the solutions occurs through diffusion processes alone. Hence, a satisfactory mixing performance generally requires the use of extended flow channels and takes longer to accomplish such that the practical benefits of such devices are somewhat limited. Consequently, accomplishing the goal of μ-TAS requires the development of enhanced mixing techniques for microfluidic structures.

Increasing the contact area of the samples to be mixed is an efficient means of promoting the diffusion effect. Previous researchers have demonstrated a variety of passive mixing techniques which enhance the diffusion process by feeding the samples through discrete via holes,[1] cantilever plate valves,[2] or multichannels.[3] Passive mixing methods using time-dependent flows generated by side channels have also been shown to increase diffusion efficiency.[4,5] The multiple folding of samples in the microchannel represents a further means to increase the contact area in passive mixing apparatus. Three-dimensional microchannels fabricated in silicon,[6−8] PDMS,[9] Mylar,[10] and PMMA[11] have been utilized for the successive lamination of samples. It has been demonstrated that samples can be mixed within 100−300 ms through multiple folding.[7] However, the dead volume trapped at the channel corners may cause concern in practical applications. Alternatively, passive mixing utilizing surface hetereogeneity was also demonstrated.[12,13] Mixing performance up to 95% can be achieved within 2.2 mm mixing length.[14]

The application of external forces to perform active fluid mixing is also a commonly applied technique. Mechanical transducers can be incorporated into microdevices using appropriate microfabrication techniques. The use of embedded PZT ultrasonic transducers to generate acoustic waves for the efficient stirring of samples in a micromixer has been successfully reported;[15,16]

* Corresponding author. Phone: +886-8-7703202-7553. Fax: +886-946526044. E-mail: loudyfu@mail.npust.edu.tw.

[†] National Sun Yat-sen University.

[‡] National Pingtung University of Science and Technology.

(1) Miyake, R.; Lammerink, T. S. J.; Elwenspoek, M.; Fluitman, J. H. J. *Proc. IEEE MEMS* **1993**, 248−253.
(2) Voldman, J.; Gray, M. L.; Schmidt, M. A. *J. MEMS* **2000**, *9*, 295−302.
(3) Koch, M.; Chatelain, D.; Evans, A. G. R.; Brunnschweiler, A. *J. Micromech. Microeng.* **2003**, *8*, 123−126.
(4) He, B.; Burke, B. J.; Zhang, X.; Zhang, R.; Regnier, R. E. *Anal. Chem.* **2001**, *73*, 1942−1947.
(5) Melin, J.; Giménez, G.; Rozhed, N.; van der Wijngaart, W.; Stemme, G. *Proc. 7th Int. Conf. Miniaturized Chem. Biochem. Anal. Syst.* **2003**, 167−170.
(6) Schwesinger, N.; Frank, T.; Wurmus, H. *J. Micromech. Microeng.* **1996**, *6*, 99−102.
(7) Branerbjerg, J.; Gravesen, P.; Krog, J. P.; Nielsen, C. R. *Proc. IEEE MEMS* **1996**, 441−446.
(8) Liu, R. H.; Stremler, M. A.; Sharp, K. V.; Olsen, M. G.; Santiago, J. G.; Adrian, R. J.; Aref, H.; Beebe, D. J. *J. MEMS* **2000**, *9*, 190−197.
(9) Beebe, D. J.; Adrian, R. J.; Olsen, M. G.; Stremler, M. A.; Aref, H.; Jo, B. H. *Mech. Ind.* **2001**, *2*, 343−348.
(10) Munson, M. S.; Yager, P. *Proc. 7th Int. Conf. Miniaturized Chem. Biochem. Anal. Syst.* **2003**, 495−498.
(11) Schönfeld, F.; Hessel, V.; Hofmann, C. *Lab Chip* **2004**, *4*, 65−69.
(12) Stroock, A. D.; Weck, M.; Chiu, D. T.; Huck, W. T. S.; Kenis, P. J. A.; Ismagilov, R. F.; Whitesides, G. M. *Phys. Rev. Lett.* **2000**, *84*, 3314−3317.
(13) Erickson, D.; Li, D. *Langmuir* **2002**, *18*, 1883−1892.
(14) Biddiss, E.; Erickson, D.; Li, D. *Anal. Chem.* **2004**, *76*, 3208−3213.
(15) Vivek, V.; Zeng, Y.; Kim, E. S. *Proc. IEEE MEMS* **2000**, 668−673.
(16) Rife, J. C.; Bell, M. I.; Horwitz, J. S.; Kabler, M. N.; Kabler, R. C. Y.; Auyeung, R. C. Y.; Kim, W. J. *Sens. Actuators, A* **2000**, *86*, 135−140.

10.1021/ac0494782 CCC: $27.50 © 2004 American Chemical Society
Published on Web 08/12/2004

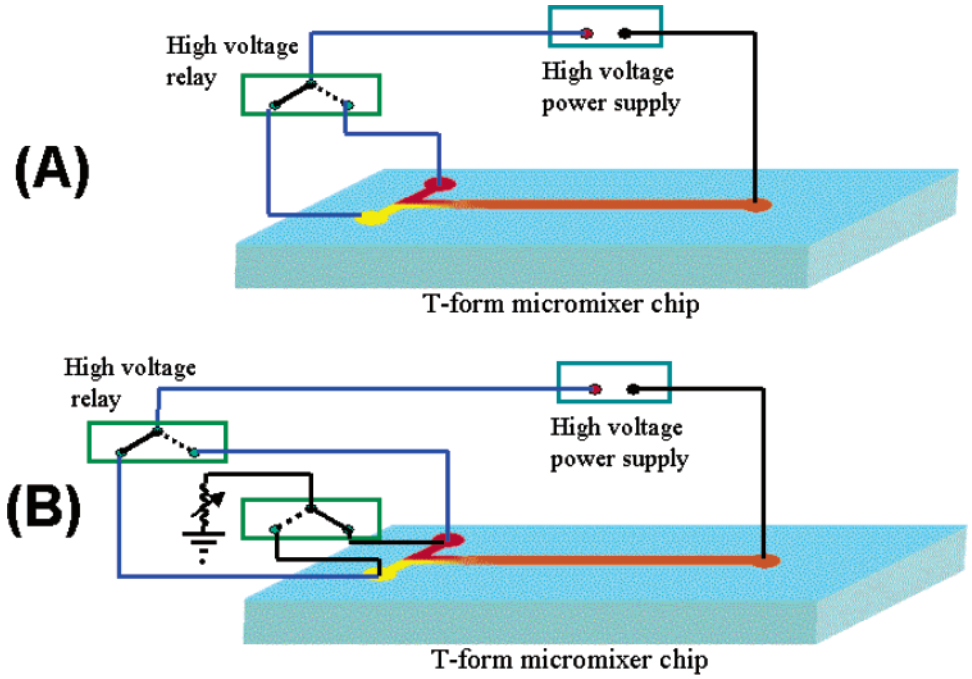

Figure 1. Schematic representations of two operation modes and system setup for present micromixer: (a) conventional switching mode and (b) pinched switching mode.

however, the acoustic vibrations induced during mixing generate heat, which can create problems when mixing biological samples. Lu et al. proposed an elaborate microdevice for microfluidic mixing in which micro magnetic stirrers were fabricated using surface micromachining techniques.[17] A 3 × 3 magnetic stirrer array was used for rapid mixing results in their study. Nevertheless, the mixing performance demonstrated in the study was not superb with this approached. Rong et al. also presented an active mixer using magnetic forces.[18] Magnetic beads were mixed with the sample fluids and were driven by pairs of integrated electromagnets. Integrated thermal bubble pumps for generating pulsatile driving forces have also been applied for the mixing of liquid samples in microfluidic devices.[19,20] Lee et al. utilized microdevices incorporating embedded microelectrodes for the dielectrophoretic stretching and folding of sample fluids.[21,22] Similarly, the use of embedded electrode pairs to create flow stream instabilities by generating localized surface energy changes has also been demonstrated as a means of achieving liquid mixing with no moving parts.[23,24]

Microfluidic devices incorporating T-form microchannels and utilizing electrokinetic forces to drive the sample fluid are widely used in a variety of bioanalytical applications, including DNA restriction,[25] multiple sample injection,[26] sample extraction, controlled fraction mixing,[27,28] etc. Developing a simple and reliable electrokinetically driven mixing method is of great practical importance. Oddy et al. presented an electrokinetically driven microfluidic mixer for the rapid stirring of two fluid streams by means of axial and orthogonal wave functions generated by a high voltage amplifier;[29] however, a very high driving voltage was required (up to 4−8 kV). Johnson et al.[30] proposed a T-form micromixer with a series of ablated wells for the rapid mixing of samples and successfully demonstrated a high mixing efficiency. Huang et al.[31] presented an electrokinetically driven micromixer using high-voltage (1700 V/cm) waveforms for stirring purposes. In addition to the sample loading channels, the micromixer also incorporated side channels to enhance the sample mixing effect; however, operating this system was complex, since it was necessary to control the voltage precisely at an increased number of microchannel locations. Finally, in a study including both numerical analysis and optical testing, Mengeaud et al.[32] analyzed Y-form micromixers with various zigzag mixing channel configurations.

This paper proposes a T-form micromixer which utilizes a switching DC field to induce electroosmotic flows for sample driving and flow instability generation. Figure 1 presents the basic operating principles of this device, which is capable of operating either in a conventional switching mode (Figure 1a) or in a novel pinched switching mode (Figure 1b). In the conventional switching mode, a driving voltage is applied to one channel only, while

(17) Lu, L. H.; Ryu, K. S.; Liu, C. *J. MEMS* **2002**, *11*, 462−469.
(18) Rong, R.; Choi, J. W.; Ahn, C. H. *Proc. 7th Int. Conf. Miniaturized Chem. Biochem. Anal. Syst.* **2003**, 335−338.
(19) Deshmukh, A. A.; Liepmann, D.; Pisano, A. P. *IEEE Proc. Solid State Sens. Actuator Workshop* **2000**, 73−76.
(20) Tsai, J. H.; Lin, L. *Sens. Actuators, A* **2002**, *97−98*, 665−671.
(21) Lee, Y. K.; Deval, J.; Tabeling, P.; Ho, C. M. *Proc. IEEE MEMS* **2001**, 483−486.
(22) Deval, J.; Tabeling, P.; Ho, C. M. *Proc. IEEE MEMS* **2002**, 36−39.
(23) Wu, H. Y.; Liu, C. H. *IEEE Proc. Solid State Sens. Actuator Workshop* **2003**, 631−634.
(24) Hau, W. L. W.; Lee, L. M.; Lee, Y. K.; Zohar, Y. *Proc. 7th Int. Conf. Miniaturized Chem. Biochem. Anal. Syst.* **2003**, 491−494.
(25) Jacobson, S. C.; Remsey, J. M *Anal. Chem.* **1996**, *68*, 720−723.
(26) Waters, L. C.; Jacobson, S. C.; Kroutchinina, N.; Khandurina, J.; Foote, R. S.; Ramsey, J. M. *Anal. Chem.* **1998**, *70*, 158−162.
(27) Jacobson, S. C.; McKnight, T. E.; Ramsey, J. M. *Anal. Chem.* **1999**, *71*, 4455−4459.
(28) Kutter, J. P.; Jacobson, S. C.; Ramsey, J. M. *Anal. Chem.* **1997**, *69*, 5165−5171.
(29) Oddy, M. H.; Santiago, J. G.; Mikkelsen, J. C. *Anal. Chem.* **2001**, *73*, 5822−5832.
(30) Johnson, T. J.; Ross, D.; Locascio, L. E. *Anal. Chem.* **2002**, *74*, 45−51.
(31) Huang, P.; Breuer, K. S. *Proc. Transducers '03* **2003**, 663−666.
(32) Mengeaud, V.; Josserand, J.; Girault, H, H. *Anal. Chem.* **2002**, *74*, 4279−4286.

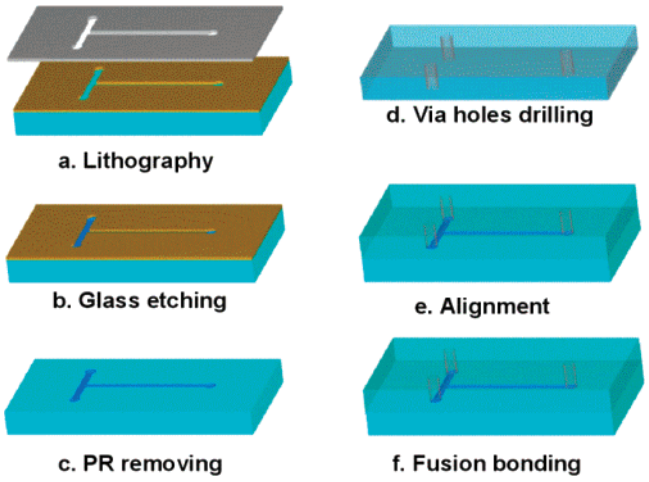

Figure 2. Overview of fabrication process for current microfluidic device.

the second channel is open. Cyclic switching of the applied voltage drives the sample fluid into the mixing channel and simultaneously generates an electrokinetic instability. In the pinched switching mode, a series of resistors are used to establish a pinch voltage during the cyclic switching of the applied voltage. Pinched switching generates greater disturbances, and, hence, provides an enhanced mixing performance. Both methods proposed in the present study perform sample loading and flow instability generation simultaneously within the same microchannel. Furthermore, the device can be operated in either mode using a single power supply. Hence, the proposed T-form microfluidic mixer is simple, stable, and reliable. This study describes the mixing characteristics of the proposed device and establishes its optimal operational settings. The mixing performance of the microfluidic device is evaluated through computer simulation, and the results are then compared to those obtained experimentally.

EXPERIMENTAL SECTION

Fabrication Process. Since the samples are to be electrokinetically driven in the present study, a silanol-group-rich material, such as glass, is preferred as the substrate material. Consequently, the present microchips were fabricated on low-cost microscope slides (25 mm × 75 mm × 1.0 mm, Marienfeld, Germany). Prior to the fabrication process, the slides were annealed at 400 °C for 4 h in order to release residual stress. The slides were then cleaned through immersion in a boiling piranha solution (concentrated sulfuric acid mixed with concentrated hydrogen peroxide in 3:1 volume ratio) for 10 min. **(Piranha solutions are extremely energetic and may result in explosion or skin burns if not handled with extreme caution.)** A simplified representation of the current fabrication process is presented in Figure 2. A detailed description of the fabrication procedure is presented in ref 33, but the basic processes can be briefly summarized as follows. Initially, a thin layer of AZ 4620 photoresist was applied onto the glass substrate and then patterned using a standard photolithography process (Figure 2a). The patterned photoresist layer was hard-baked and then used directly as a mask in the etching of the glass substrates in a commercially available buffered HF (buffered oxide etchant, J. T. Baker) for 45 min (Figure 2b). The etched glass substrates were then immersed in a diluted KOH solution (KOH (45%)/DI = 1:9, 80 °C) to remove the photoresist layer (Figure 2c). Meanwhile, holes for fluid loading were drilled in a second bare glass slide using a diamond drill bit of diameter 1.5 mm (Figure 2d). Both glass substrates were cleaned in a boiling piranha solution and then carefully aligned (Figure 2e). Finally, the substrates were fusion-bonded in a sintering oven at a temperature of 580 °C for 10 min (Figure 2f). The entire fabrication process lasted no longer than 10 h. The wings of the completed fabricated T-form microfluidic device measured 1 cm in length, and the main mixing channel length was 4 cm. The widths and depths of the various microchannels were 100 and 40 μm, respectively.

Experimental Procedure. The experimental tests were performed under a fluorescence microscope (E-400, Nikon, Japan) using a mercury lamp module for fluorescein excitation. A CCD module (DXC-190, Sony, Japan) with a high-speed image acquisition interface (DVD PKB, V-gear, Taiwan) was used to acquire the optical images. The two liquid samples were in the form of a 1 mM sodium borate buffer (pH = 9.2) and a sodium borate buffer with 10^{-4} M Rhodamine B fluorescence dye, respectively. The samples were driven by a programmable high-voltage power supply (MP-3500, Major Science, Taiwan) capable of high-speed switching frequencies of up to 10 Hz. In the conventional switching mode (Figure 1a), the high-voltage power supply controlled the relay such that the applied driving voltage alternated from one sample reservoir to the other. This operation mode automatically maintains the interface of the two sample liquids at the center of the T-junction. In the pinched switching mode (Figure 1b), the pinched voltages were established by connecting resistors of 50, 100, 150, and 200 MΩ between the two sample reservoirs and a common ground. It is noted that the high-ohm resistors were formed of a series of individual 10-MΩ metallic film resistors.

The mixing performance was evaluated by analyzing the experimental images using digital image processing techniques. The captured color images were converted into corresponding gray scale images for a better indication of the fluorescence intensity. It was assumed that the gray scale value of an image corresponded to the particular concentration level of the fluorescence dye. Hence, the gray scale value for a channel filled with fluorescence dye was specified as 1, whereas that of a channel empty of dye was specified as 0. To determine the concentration distribution within the mixing channel, the corresponding gray scale values were measured and normalized at cross sections located at various distances downstream from the T-junction. At each cross section, 10 discrete measurements were made across the width of the 100-μm-wide channel. The acquired experimental values were then compared with the numerical results.

MATHEMATICAL MODEL

This paper focuses primarily on predicting the electroosmotic flow in the T-form micromixer under different operation modes and operating parameters. Once an electrical field is applied to a microchannel, the transient process of establishing electroosmotic flow has a duration of no more than a few hundred microseconds and is dependent on the microchannel dimensions and on the ionic concentrations of the buffer.[34] This duration is typically much shorter than the related characteristic times for injecting, separat-

(33) Lin, C. H.; Lee, G. B.; Lin, Y. H.; Chang, G. L. *J. Micromech. Microeng.* **2001**, *11*, 726−732.

ing, or mixing, etc. Thermal effects can also be neglected since the dissipation capability of a microfluidic chip is sufficiently high that no joule heating effect is observed for electrical fields of up to 800 V/cm.[35,36] To further simplify the governing equation, the following assumptions have been made: (1) no chemical reactions, (2) the aqueous electrolyte solution is Newtonian and incompressible, (3) the gravitational effect is negligible, (4) the diffusion coefficient is constant, and (5) the joule heating effect is negligible.

Modeling the present microfluidic device requires solving the electrical potential, pressure, velocity components, and sample concentration throughout the computational domain. The current authors have previously developed physical models[37−39] based on (a) the Poisson equation for the electrical potential and ζ potential, (b) the Nernst−Planck equations for the ionic concentration, (c) the full Navier−Stokes equations modified to include the effects of the body force due to the electrical and charge densities, and (d) a concentration equation for the sample plug distribution.

The physical model developed in the present study combines the Poisson equations for the applied electrical potential and ζ potential of the fluid−solid boundary with the ionic concentrations (n^+, n^-) of the positive and negative ions of the fluid and the full Navier−Stokes equations modified to include electrokinetic force effects. By introducing the reference quantities L_{ref}, U_{ref}, p_{ref}, ρ_{ref}, and defining $\overline{\rho_e} = \rho_e/n_0ze = (n^+ - n^-)/n_0$, $\bar{\psi} = ze\psi/k_bT$, $\bar{t} = tU_{ref}/L_{ref}$, $\bar{u} = u/U_{ref}$, $\bar{v} = v/U_{ref}$, $\bar{x} = x/L_{ref}$, $\bar{y} = y/L_{ref}$, $\bar{p} = (p - p_{ref})/(\rho U_{ref}^2)$, $\bar{\rho} = \rho_f/\rho_{ref}$, $\overline{n^+} = (n^+ - n_0)/n_0$, $\overline{n^-} = (n^- - n_0)/n_0$, the dimensionless form of the governing equations after dropping the head symbols can be written as

$$\frac{\partial^2\psi}{\partial x^2} + \frac{\partial^2\psi}{\partial y^2} = -\frac{\kappa^2}{2}\rho_e \tag{1}$$

$$\frac{\partial n^{\pm}}{\partial t} + u\frac{\partial n^{\pm}}{\partial x} + v\frac{\partial n^{\pm}}{\partial y} = \frac{1}{ScRe}\left(\frac{\partial^2 n^{\pm}}{\partial x^2} + \frac{\partial^2 n^{\pm}}{\partial y^2}\right) \pm \frac{1}{ScRe}\left[\frac{\partial}{\partial x}\left(n^{\pm}\frac{\partial\psi}{\partial x}\right) + \frac{\partial}{\partial y}\left(n^{\pm}\frac{\partial\psi}{\partial y}\right)\right] \tag{2}$$

$$\frac{\partial u}{\partial x} + \frac{\partial v}{\partial y} = 0 \tag{3}$$

$$\frac{\partial u}{\partial t} + u\frac{\partial u}{\partial x} + v\frac{\partial u}{\partial y} = -\frac{\partial p}{\partial x} + \frac{1}{Re}\left(\frac{\partial^2 u}{\partial x^2} + \frac{\partial^2 u}{\partial y^2}\right) - \mathrm{Gx}\rho_e\frac{\partial\psi}{\partial x} \tag{4}$$

$$\frac{\partial v}{\partial t} + u\frac{\partial v}{\partial x} + v\frac{\partial v}{\partial y} = -\frac{\partial p}{\partial y} + \frac{1}{Re}\left(\frac{\partial^2 v}{\partial x^2} + \frac{\partial^2 v}{\partial y^2}\right) - \mathrm{Gx}\rho_e\frac{\partial\psi}{\partial y} \tag{5}$$

$$\frac{\partial C}{\partial t} + u\nabla C = \frac{1}{ScRe}\nabla^2 C \tag{6}$$

In the equations above, $\kappa = W \times K$, where K is the Debye−Huckel parameter given by $K = (2n_0z^2e^2/\epsilon\epsilon_0k_BT)^{1/2}$; $1/K$ is the characteristic thickness of the charge density; $\rho_e = (n^+ - n^-)ze$ is the charge density; n^+ and n^- are the respective concentrations of the positive and negative ions; ϵ is the dielectric constant of the medium; ϵ_0 is the permittivity of a vacuum; n_0 is the bulk concentration of the ions; k_B is the Boltzmann constant; T is the absolute temperature; $L_{ref} = W$, where W is the channel height; $U_{ref} = \psi_{inlet}\epsilon\epsilon_0|\zeta|/\mu L$, where ψ_{inlet} is the activated potential at the inlet; Re is the Reynolds number given by $Re = \rho_f U_{ref}L_{ref}/\mu = \rho_f(\psi_{inlet}\epsilon\epsilon_0|\zeta|/\mu L)(L_{ref}/\mu)$; Sc is the Schmidt number given by $Sc = \mu/\rho_f D_i$; μ is the liquid viscosity; ρ_f is the fluid density; D_i is the diffusion coefficient of the sample; ζ is the surface ζ potential; p is the pressure; Gx is the ratio of the EDL energy to the mechanical kinetic energy and is given by $\mathrm{Gx} = 2n_0k_BT\rho_fW^2/\mu Re^2$; and finally, C is the sample concentration. Note that the initial conditions, the boundary conditions, and details of the present numerical method are fully presented in ref 40.

The present simulations assumed a silica-based microchannel and a sodium borate buffer fluid. The values of the physical and electrical properties of this buffer are listed as follows.

dielectric constant, $\epsilon = 80$
initial ζ potential of the channel wall, $\zeta = -75$ mV
fluid viscosity, $\mu = 10^{-3}$ N·s/m^2
electrolyte concentration, $c = 10^{-1}$ mM
Schmidt number of charge density, $Sc = 10^5$
applied longitudinal electrical field, ∼50 to 300 V/cm
diffusion coefficient of sample (Rhodamine B), $D = 10^{-10}$ m^2/s

RESULTS AND DISCUSSION

(a) Laminar Flow. Figure 3 presents the numerical and experimental results for the case of steady flow in the microfluidic channel under a driving voltage of 90 V/cm. Figure 3a and b indicates the normalized electrical potential and the corresponding fluid flow streamlines around the T-junction. Figure 3c shows the simulated concentration distributions of the two species in the microfluidic channel. Although natural diffusion of the two samples generates a localized mixing phenomenon at the sample interface, the mixing performance is very limited. Figure 3d presents the experimental results for the steady flow condition. The laminar flow pattern observed experimentally is virtually identical to the simulation result. This flow pattern is a clear indication that the T-form channel provides an inefficient sample mixing performance.

(b) Conventional Switching Mode. In the conventional switching mode, the driving voltage is applied alternately first to one inlet reservoir and then to the other. Importantly, when the driving voltage is applied to one inlet, the second inlet remains open. Figure 4 presents the potential distributions and streamlines for the two steps of this switching mode. As shown in Figure 4a, a floating voltage is established at the open inlet with a ratio of 0.83 to the applied voltage. Figure 4b shows that the presence of this floating voltage prevents the fluid exiting from the voltage-applied channel from entering the open inlet. Therefore, in the conventional switching mode, the fluids from the two inlet channels flow alternatively into the mixing channel. This increases the flow instability and increases the contact area of the two fluid samples. Consequently, the diffusion phenomena acting within the two liquids are enhanced.

Figure 5 presents the simulated and experimental flow contours for the conventional switching mode obtained when applying switching frequencies in the range 1−10 Hz and a constant driving voltage of 90 V/cm. The green regions in the simulation results

(34) Dose, E. V.; Guiochon, G. *J. Chromatogr., A* **1993**, *652*, 263−275.
(35) Jin, Y.; Luo, G. A.; Tang, Y. H.; Zhou, Z. Y. *J. Anal. Sci.* **2001**, *17*, 148−152.
(36) Erickson, D.; Sinton, D.; Li, D. *Lab Chip* **2003**, *3*, 141−149.
(37) Fu, L. M.; Yang, R. J.; Lee, G. B.; Liu, H. H. *Anal. Chem.* **2002**, *74*, 5084−5091.
(38) Fu, L. M.; Yang, R. J.; Lee G. B. *Anal. Chem.* **2003**, *75*, 1905−1910.
(39) Fu, L. M.; Lin, C. H. *Anal. Chem.* **2003**, *75*, 5790−5796.
(40) Fu, L. M.; Yang, R. J.; Lee G. B. *J. Sep. Sci.* **2002**, *25*, 996−1010.

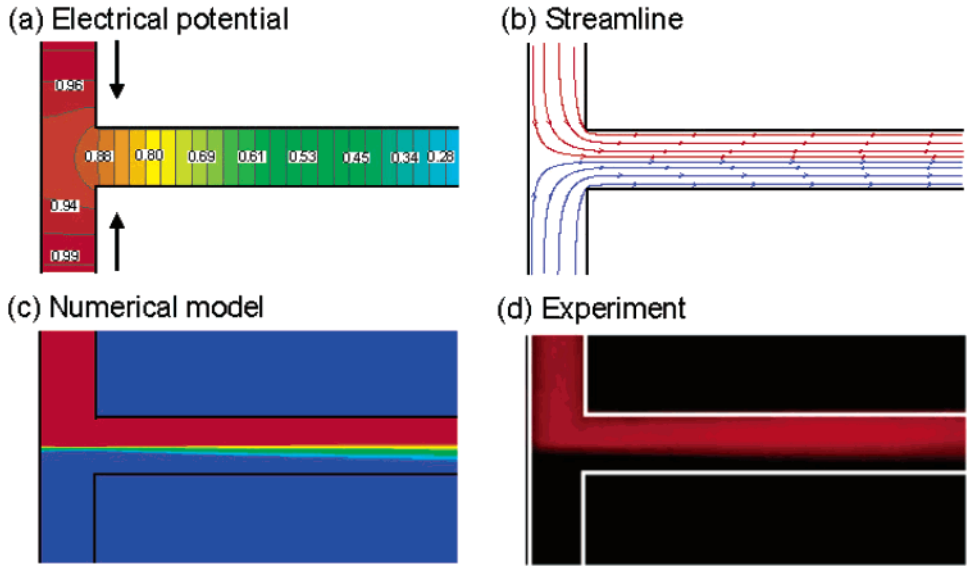

Figure 3. Numerical and experimental results for steady flow in microfluidic channel: (a) electrical potential distribution, (b) streamlines, (c) numerical model for flow contours, and (d) experimental image captured using CCD.

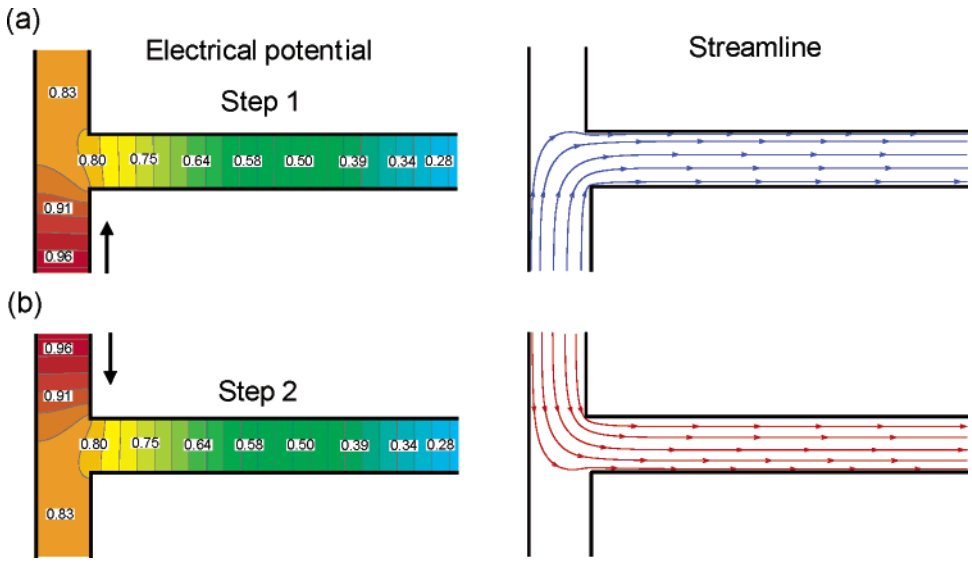

Figure 4. (a) Electrical potential distributions and (b) streamlines in conventional switching mode.

represent areas of fluid mixing. As shown in both sets of figures, at low switching frequencies (1−4 Hz), the periodic injection of sample plugs into the mixing channel results in a waveform flow along the length of the mixing channel. Compared to the case of laminar flow presented above, these waveform flow patterns increase the contact area of the two samples and, hence, generate a more rapid diffusion effect. In general, a greater contact area can be obtained at a higher switching voltage, since the wavelength is shorter. However, as shown in Figure 5d and e for switching voltages of 6 and 10 Hz, respectively, the amplitudes of the waves decrease with increasing frequency, and therefore, the mixing effect is lessened.

For different values of switching frequency, Figure 6 presents the variation in normalized concentration intensity across the width of the microchannel at a cross section located 1000 μm downstream from the T-junction. The values "1.0" and "0" on the y axis refer to the concentration intensities of the pure fluorescence dye and the pure buffer, respectively. Meanwhile, the value of "0.5" indicates a fully mixed concentration. Hence, a horizontal line at $y = 0.5$ represents a complete mixing of the two samples across the width of the microchannel. In Figure 6, the lines indicate the simulation results, and the symbols plot the experimental data. Note that in this figure, the experimental images are obtained by mercury-lamp-induced fluorescence, fluorescence intensities are given in arbitrary units, and the values are normalized. Meanwhile, the gray scale in the numerical simulation images represents the concentration distribution normalized relative to the initial (maximum) sample concentration. It is noted that the curves for low-frequency conditions (1 and 2 Hz) are not fixed, but change periodically as the fluorescence plugs pass the detection region. The concentration intensity profiles attain a stable status when the switching frequency exceeds 4 Hz. As shown in Figure 6, a higher switching frequency yields a flatter curve.

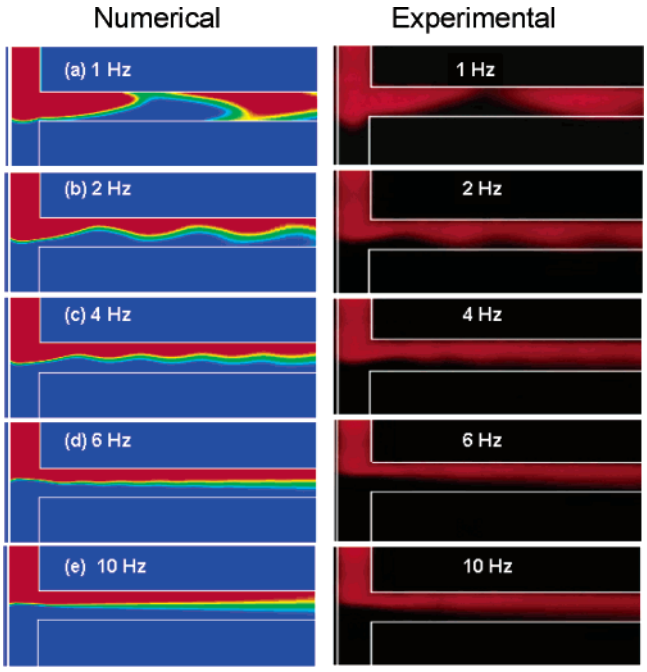

Figure 5. Numerical and experimental results for flow contours in conventional switching mode at different switching frequencies.

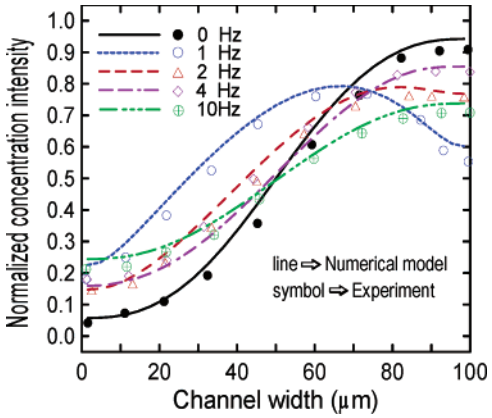

Figure 6. Variation in normalized concentration intensity across channel width at microchannel cross section located 1000 μm downstream from the T-junction at different switching frequencies.

A mixing efficiency parameter, σ, can be defined[13] as

$$\sigma = \left(1 - \frac{\int_0^W |C - C_\infty| \, dy}{\int_0^W |C_0 - C_\infty| \, dy}\right) \times 100\%$$

where C is the species concentration profile across the width of the mixing channel, and C_0 and C_∞ are the species concentrations in the completely unmixed (0 or 1) and completely mixed states (0.5), respectively.

Figure 7 demonstrates the mixing efficiency of the proposed micromixer when operated in conventional switching mode at different switching frequencies. Note that for reasons of clarity, the numerical and experimental curves are plotted for only some of the tested frequencies. The experimental data were measured at positions between 300 and 1200 μm downstream from the T-junction. Under laminar flow conditions, natural diffusion results

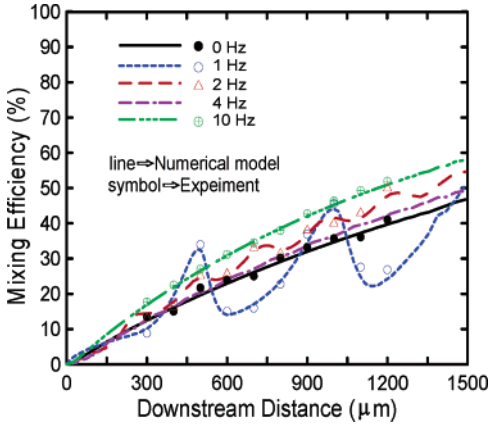

Figure 7. Mixing efficiency at different switching frequencies in conventional switching mode.

in a maximum mixing efficiency of 47%. The results of Figure 7 reveal that the maximum mixing efficiency obtained in the conventional switching mode is <60%; therefore, this particular operation mode fails to enhance the mixing efficiency significantly. This failing can likely be attributed to the limiting of the sample switching amplitude by the floating voltages established in the open inlets.

(c) Pinched Switching Mode. To increase the mixing efficiency of the T-form microfluidic mixer, a simple technique is developed in which a lower voltage is established at the open inlet channel by connecting a series of high-ohm resistors between the reservoirs and the ground end (Figure 1b). A lower pinched voltage forces the sample fluid flow into the open inlet and increases the switching amplitude. Figure 8 shows the electrical potential distributions and corresponding streamlines for a pinched switching mode operation using a 200-MΩ resistor. The fluid from the driven inlet flows not only into the mixing channel but also partially into the open inlet, as shown in Figure 8b. However, when the direction of the driving electric field reverses as the applied voltage switches to the other inlet, the fluid which previously flowed into the open inlet is expelled. Hence, cyclic switching generates a continuous large-amplitude waveform flow in the mixing channel.

Figure 9 shows the numerical and experimental flow contours for different switching frequencies under the pinched switching mode using a constant driving voltage of 90 V/cm and a 200-MΩ resistor. Since the liquid sample from the driven channel partially enters the open channel and is then pushed back, the wavelengths of the generated waves are shorter than those in the conventional switching mode and have a larger amplitude. Hence, the pinched switching mode ensures an enhanced mixing efficiency. As shown in Figure 9c, the two samples are almost fully mixed at a switching frequency of 4 Hz; however, as the switching frequency increases, the amplitude of the waves decreases, thereby causing a reduction in the mixing efficiency. It is thought that the decrease in wave amplitude can be attributed to the moment of inertia effect of the liquid; therefore, simply increasing the switching frequency does not absolutely guarantee an improved mixing performance. Furthermore, in our tests, it shown that the resistor value (50, 100, 150, or 200 MΩ) appeared to have little effect on the efficiency of the mixing performance.

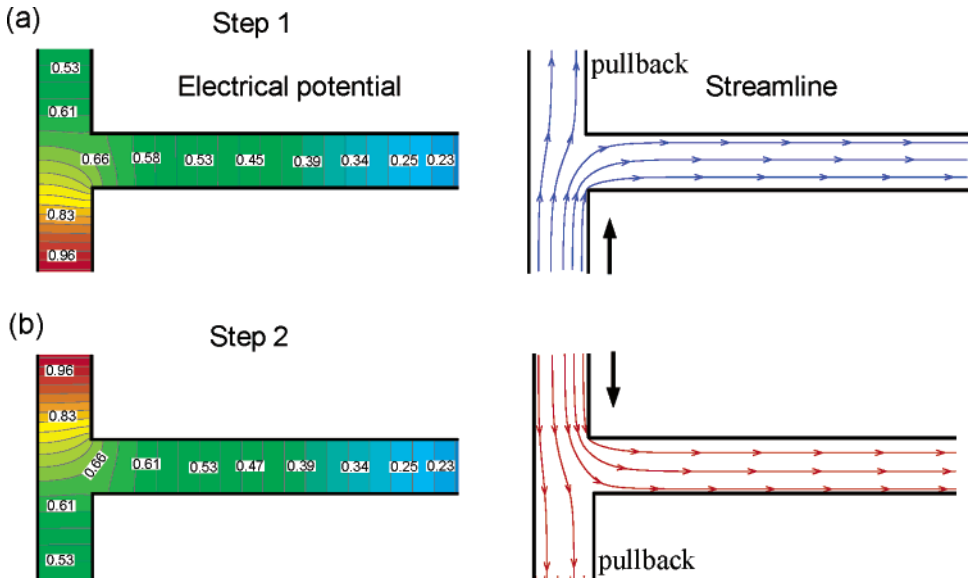

Figure 8. Electrical potential distributions and streamlines in pinched switching mode operation.

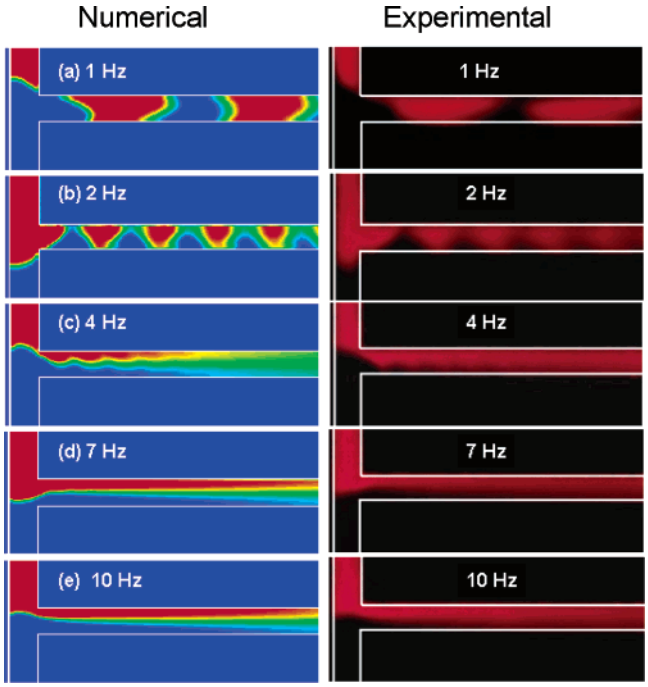

Figure 9. Numerical and experimental flow contours at different switching frequencies in pinched switching mode operation.

Figure 10 demonstrates the mixing efficiency of the microfluidic mixer when operated in pinched switching mode. At low switching frequencies of 1 and 2 Hz, the mixing efficiency exhibits waveformlike curves, which are indicative of the periodic flow of the fluorescence samples into the mixing channel. When the switching frequency is increased to 4 Hz, a mixing efficiency of 97% is achieved within a 1-mm distance downstream from the T-junction. Although omitted from the figure for reasons of clarity, the simulation and experimental results revealed that mixing efficiencies of 87 and 80% were obtained at the equivalent location for switching frequencies of 5 and 6 Hz, respectively. Therefore, it is clear that the proposed pinched switching mode significantly enhances the mixing performance of the micromixer.

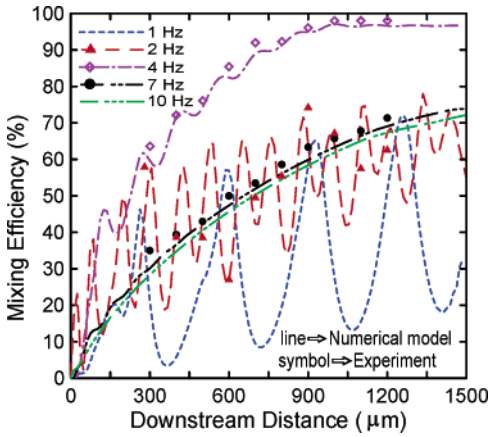

Figure 10. Mixing efficiency of micromixer in pinched switching mode operation.

(d) Optimization of Pinched Switching Mode. As discussed in the previous sections, the switching frequency has a significant influence on the mixing performance. However, it is known that the mixing performance is also influenced by the magnitude of the applied driving voltage. Under electrokinetic driving conditions, the sample flows through the microchannel more rapidly when a higher driving voltage is applied. The application of high driving voltages increases the fluid flow disturbance, but it also reduces the contact time between the two samples within a certain distance, since the flow speed is faster. Therefore, it is necessary to investigate the interrelationships between driving voltage, switching frequency, and mixing performance. Using driving voltages of 60, 90, 120, and 180 V/cm and resistors of 200 MΩ at both sample reservoirs, the mixing efficiency was determined numerically and experimentally at different values of switching frequency. The corresponding results are presented in Figure 11. As before, the mixing performance was determined at a location of 1 mm downstream from the T-junction. As discussed in Section b, the mixing efficiency does not always increase with increasing switching frequency, since the wave amplitude is reduced at higher frequencies. Furthermore, it is observed that the mixing performance is not necessarily enhanced by an increased driving

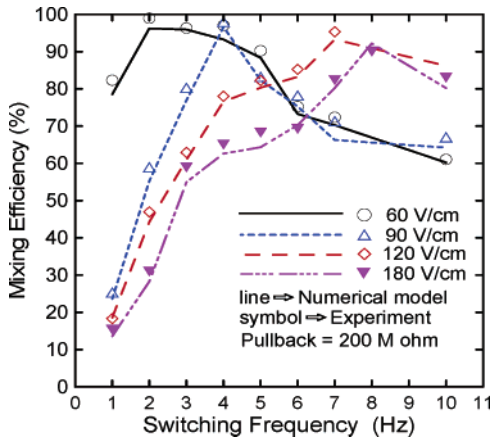

Figure 11. Numerical and experimental evaluations of mixing efficiency at different driving voltages and switching frequencies.

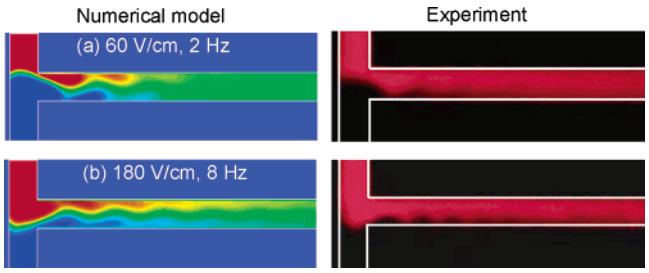

Figure 12. Flow contours for two optimized operating conditions at low and high driving voltages.

voltage, since the mixing time is reduced at higher driving voltages. This effect is of benefit in practical applications, since the system can be operated under a lower driving voltage.

The present results indicate that a maximum mixing efficiency of 97% is obtained within 1 mm of the T-junction for a driving voltage of 60 V/cm in 2.5 s and a switching frequency of 2 Hz. Although this performance satisfies the requirements of most practical applications, a higher throughput may be required in certain applications. The sample flow velocity appears to have a linear relationship with the applied electric gradient for electrokinetically driven liquid samples. The optimized operating conditions for the current micromixer under different driving voltages are presented in Figure 11. The optimal mixing efficiency for all the tested cases can be larger than 90%, which indicates the feasibility of this micromixer.

Figure 12 presents the flow contours for optimized operating conditions in the cases of low and high driving voltages. In the low driving voltage case of 60 V/cm, the maximum mixing efficiency is found to be 97% at a switching frequency of 2 Hz. Meanwhile, for a high driving voltage of 180 V/cm, the maximum mixing efficiency can reach 90% within 2 s at a switching frequency of 8 Hz. Although a higher electrical gradient can mix samples with a greater throughput at higher switching frequencies, the switching frequency of the present power supply is limited to 10 Hz. Moreover, it is uneconomical to adopt this approach when lower driving voltages and switching frequencies can provide an equally acceptable mixing performance.

CONCLUSIONS

This study has proposed an active T-form microfluidic mixer utilizing switching electroosmotic flow. The micromixer can operate in either a conventional switching mode or in a pinched switching mode to perform electrokinetically driven mixing. A numerical model has been used to analysis the electrical potential and streamline distributions in the micromixer. The mixing performance of the device in its two operation modes has been evaluated both numerically and experimentally. The mixing efficiency obtained in the conventional operation mode is of the order of 45−60% at a position of 1 mm downstream from the T-junction. This rather unsatisfactory performance may not meet the requirements of certain applications and is likely caused by the floating voltages in the open inlets, which limit the switching amplitudes of the fluid samples; however, the novel pinched switching method significantly improves the mixing performance and develops a mixing efficiency of 97%. This study has also investigated the optimal operating conditions for the pinched switching mode in terms of the switching frequency and driving voltage parameters. Under a very low driving voltage of 60 V/cm, a switching frequency of 2 Hz is sufficient to provide a high mixing efficiency within a short mixing distance. Moreover, this high performance micromixer requires no moving parts and involves a simple fabrication process The results of the present study provide a valuable contribution to the future development of a variety of applications in the micro total analysis systems field.

ACKNOWLEDGMENT

The current authors appreciate the financial support provided to this study by the National Science Council of Taiwan under Grants Nos. NSC 93-2320-B-110-006 and NSC 93-2320-B-020-001.

SUPPORTING INFORMATION AVAILABLE

A movie is provided. This material is available free of charge via the Internet at http://pubs.acs.org.

Note Added after ASAP. Paper was originally posted on the Web on August 12. Supporting Information was added on August 20 and the paper was reposted.

Received for review April 5, 2004. Accepted July 2, 2004.

AC0494782